Lolium latent virus (*Alphaflexiviridae*) coat proteins: expression and functions in infected plant tissue

Anna Maria Vaira,[1,2]† Hyoun-Sub Lim,[3]† Gary R. Bauchan,[4] Robert A. Owens,[5] Angela Natilla,[5] Margaret M. Dienelt,[2] Michael D. Reinsel[2] and John Hammond[2]

Correspondence
John Hammond
John.Hammond@ars.usda.gov

[1]Istituto di Virologia Vegetale CNR, Strada delle Cacce 73, 10135, Torino, Italy

[2]USDA-ARS, USNA, Floral and Nursery Plants Research Unit, 10300 Baltimore Avenue, Beltsville, MD, USA

[3]Department of Applied Biology, Chungnam National University, Daejeon, 305-764, Republic of Korea

[4]USDA-ARS, PSI, Electron and Confocal Microscopy Unit, 10300 Baltimore Avenue, Beltsville, MD, USA

[5]USDA-ARS, PSI, Molecular Plant Pathology Laboratory, 10300 Baltimore Avenue, Beltsville, MD, USA

The genome of *Lolium latent virus* (LoLV; genus *Lolavirus*, family *Alphaflexiviridae*) is encapsidated by two carboxy-coterminal coat protein (CP) variants (about 28 and 33 kDa), in equimolar proportions. The CP ORF contains two 5′-proximal AUGs encoding Met 1 and Met 49, respectively promoting translation of the 33 and 28 kDa CP variants. The 33 kDa CP N-terminal domain includes a 42 aa sequence encoding a putative chloroplast transit peptide, leading to protein cleavage and alternative derivation of the approximately 28 kDa CP. Mutational analysis of the two in-frame start codons and of the putative proteolytic-cleavage site showed that the N-terminal sequence is crucial for efficient cell-to-cell movement, functional systemic movement, homologous CP interactions and particle formation, but is not required for virus replication. Blocking production of the 28 kDa CP by internal initiation shows no major outcome, whereas additional mutation to prevent proteolytic cleavage at the chloroplast membrane has a dramatic effect on virus infection.

Received 19 March 2012
Accepted 8 May 2012

INTRODUCTION

Alphaflexiviruses have flexuous virions of 470 to >800 nm in length, and the viral capsid of all previously characterized species is composed of a single polypeptide. *Lolium latent virus* (LoLV) is a recently described alphaflexivirus for which a new genus, *Lolavirus*, has been created (Adams *et al.*, 2012). LoLV infects graminaceous species and the model dicot plant *Nicotiana benthamiana*, and has a unique feature among alphaflexiviruses: the presence of two carboxy-coterminal coat protein (CP) forms in the virus particle, in essentially equimolar amounts (Vaira *et al.*, 2008). A second LoLV isolate, from the UK (Li *et al.*, 2008), shares the same characteristic (R. Li, personal communication), suggesting that the presence of two CPs in the virion is a species feature.

Several plant viruses contain two different CPs; such virions are generally composed of a major and a minor CP, with the minor CP being involved in virion assembly/stability or vector interaction. The two CPs can be expressed from different ORFs, as in comoviruses, fabaviruses and closteroviruses (Satyanarayana *et al.*, 2004).

Carboxy co-terminal CP variants have also been reported. A brome mosaic virus (BMV) isolate (ATCC66; infecting both graminaceous and dicot hosts, as does LoLV) has been described (Mise *et al.*, 1992), in which a truncated CP was encapsidated in virions together with the wild-type (WT) CP; nevertheless, in other BMV isolates only one CP type was detected, and the occurrence of two CP forms cannot be considered characteristic of BMV.

Within the genus *Marafivirus*, maize rayado fino virus (MRFV) and oat blue dwarf virus each produce carboxy-coterminal CPs (Hammond & Hammond, 2010; Hammond & Ramirez, 2001). Within the family *Betaflexiviridae*, peach chlorotic mottle virus (PCMV; genus *Foveavirus*) utilizes AUA as an upstream CP alternative start codon in addition to a supplementary in-frame downstream AUG; both CPs

†These authors contributed equally to this work.

A supplementary table is available with the online version of this paper.

are expressed in infected tissues (James *et al.*, 2007). Among the family *Alphaflexiviridae* (which includes LoLV), the presence of two conserved in-frame AUGs has been reported for the CP of *Plantago asiatica* mosaic virus (PlAMV; genus *Potexvirus*) (Ozeki *et al.*, 2009); however, the virus is thought to have a single type of CP (Solovyev *et al.*, 1994) with the first AUG as the major initiation codon for CP translation. Foxtail mosaic virus (FoMV; genus *Potexvirus*) is also able to infect graminaceous and dicot hosts. A variant of FoMV CP (ORF5) with a 48 aa 5′-terminal extension is encoded by ORF5A, which initiates upstream of the CP subgenomic RNA (Robertson *et al.*, 2000). ORF5A protein has been identified in infected tissue and protoplasts, but not in purified virions (Bruun-Rasmussen *et al.*, 2008; Robertson *et al.*, 2000).

In this report we focus on the N-terminal region differentiating the two forms of LoLV CP. This region contains multiple determinants affecting LoLV assembly and movement.

RESULTS AND DISCUSSION

Infectivity of cloned LoLV cDNAs

Three of seven pTOPO-based and two of six pUC18-based full-length LoLV genome clones (Fig. 1a, b) were infectious. At 20 days post-inoculation (p.i.), the plants inoculated with transcripts of each of these clones showed chlorotic local lesions and systemic mosaic typical of the parental virus (Fig. 1b, right panel). RT-PCR of total RNA extracted from young leaves confirmed virus replication, and two CPs of about 28 and 33 kDa were detected by Western blotting from total protein extracts, consistent with the size of CPs detected in control LoLV-infected *N. benthamiana* plants (Fig. 1b).

Analysis of the LoLV CP ORF

The ORF encoding the LoLV CP is predicted to be 882 nt long, encoding a 293 aa protein with a predicted molecular mass of about 31.6 kDa (apparent mobility 33 kDa). A second in-frame AUG is present 141 bases after the first AUG in a better translation context (Joshi *et al.*, 1997), and would yield a protein of about 26.9 kDa (apparent mobility 28 kDa). As plant viral proteins tend to mimic eukaryotic proteins, we submitted the 293 aa LoLV CP sequence to several amino acid sequence-based predictors. TargetP identified the chloroplast as the target site of the 33 kDa CP, and identified a chloroplast transit peptide (cTP) with a reliability coefficient of 1 (i.e. very reliable); ChloroP 1.1 yielded similar results, with a prediction score of 0.556 (strong) (Emanuelsson *et al.*, 2007). The predicted length of the cTP is 42 aa, with a predicted cleavage site (PV/AT) 6 aa before M49, encoded by the second ATG (Fig. 1c).

Similar results were obtained with additional protein-localization prediction programs (data not shown), indicating the presence of a functional domain in the N-terminal domain unique to the 33 kDa CP that has not been demonstrated for other flexuous viruses. To examine the functions of this putative N-terminal cTP domain in systemic movement and particle formation, a series of mutations were introduced into an infectious clone of LoLV.

Mutational analysis reveals that the cTP/N-terminal sequence is strictly required for systemic infection

Capped RNA transcripts of the WT full-length infectious clone (FL) or mutants with either ATG1 (K1) or ATG2 (K2) mutated to TTG (Fig. 1c) were inoculated separately to *N. benthamiana* plants, and symptom appearance was monitored in three independent experiments. FL and K2 plants showed clear systemic symptoms (mosaic and vein netting) at about 15 days p.i., while upper leaves of K1 plants remained symptomless. Symptom expression remained the same at 28 days p.i. and samples were collected for RNA and protein extraction. Virus replication was monitored by one-step RT-PCR with LoLV-specific primers and was detected in leaves of FL and K2 plants with systemic symptoms, but only in inoculated leaves of K1 plants. No virus replication was detected in upper leaves of K1-inoculated plants at 28 days p.i. (Fig. 2a). As expected, Western blot analysis using LoLV-specific antiserum revealed that only the 28 kDa CP was produced in low amounts in local lesions of K1-inoculated plants. No CP was detectable in upper leaves of these plants. Only the 33 kDa CP was produced at significant levels in young, symptomatic leaves of K2-inoculated plants (Fig. 2b).

Naturally occurring reversion mutants of LoLV K1 are able to re-establish systemic infection

In the absence of systemic infection, we transmitted LoLV-K1 infection mechanically from local lesions produced on inoculated leaves. The presence of the 28 kDa CP in these tissue samples was assessed by Western blotting. In a first experiment, four consecutive passages (I–IV) at about 30 day intervals were performed. Following the first mechanical transmission, surprisingly, mosaic and vein netting began to appear on young leaves of a branch of one plant (passage I) at 76 days p.i. This plant was checked immediately by RT-PCR and by Western blotting; virus replication was detected in young symptomatic leaves and a CP of the unexpected apparent size of about 31 kDa, as well as a minor amount of 28 kDa, was detected. All plants from passages I–IV were tested by RT-PCR at 94, 69, 47 and 18 days p.i., respectively, and all of them showed virus replication in young leaves; only the original plants inoculated by transcripts remained systemically uninfected (last test at 245 days p.i.). A second experiment showed similar results.

The CP region was RT-PCR-amplified and sequenced from all plants showing systemic symptoms. This analysis revealed that three different types of point mutation could

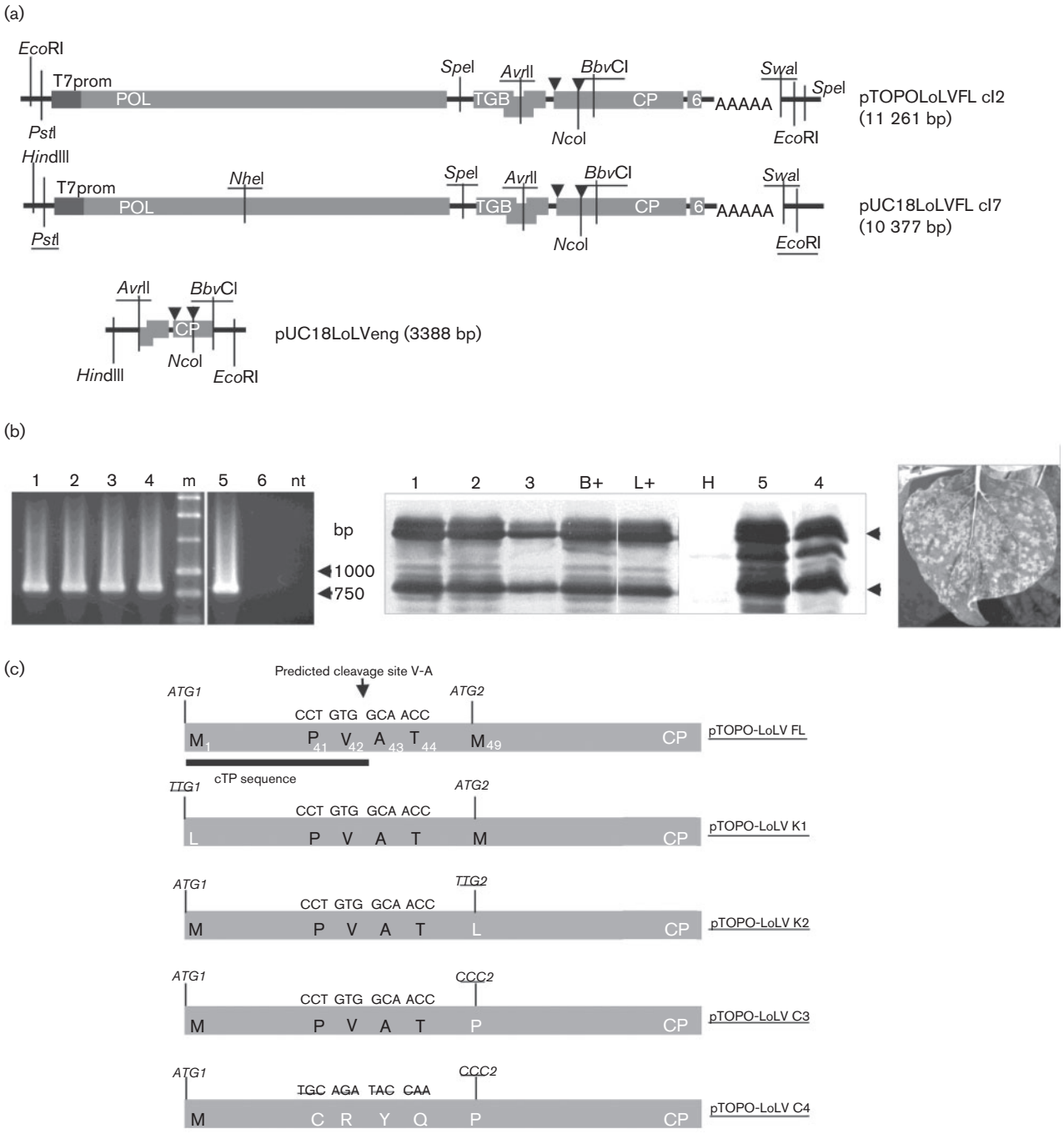

Fig. 1. (a) Schematic diagrams of LoLV infectious clones and pUC-based construct used for mutations. Unique restriction sites are underlined. Arrowheads indicate the two CP ATG sites. (b) RT-PCR of total RNA (left panel) and Western blotting of total protein extracts (central panel) from young leaves of *N. benthamiana* inoculated with RNA transcripts of infectious clones (about 14 days p.i.). RT-PCR: the expected amplicon is 806 bp; arrows indicate relevant marker sizes. Western blotting: arrows indicate the 33 and the 28 kDa CPs. Systemic symptoms (right panel) on *N. benthamiana* inoculated with pUC-LoLV-FL-cl1 transcripts (52 days p.i.). Lanes: 1, pTOPO-LoLV-FL-cl2; 2, pTOPO-LoLV-FL-cl7; 3, pTOPO-LoLV-FL-cl20; 4, pUC-LoLV-FL-cl1; 5, pUC-LoLV-FL-cl7; 6, mock-inoculated *N. benthamiana*; m, size markers; nt, no-template PCR; B+, LoLV-infected *N. benthamiana*; L+, LoLV-infected lolium; H, healthy *N. benthamiana*. (c) Scheme of mutations engineered in the N-terminal domain of LoLV CP; pTOPO-LoLV-FL is the WT infectious cDNA clone.

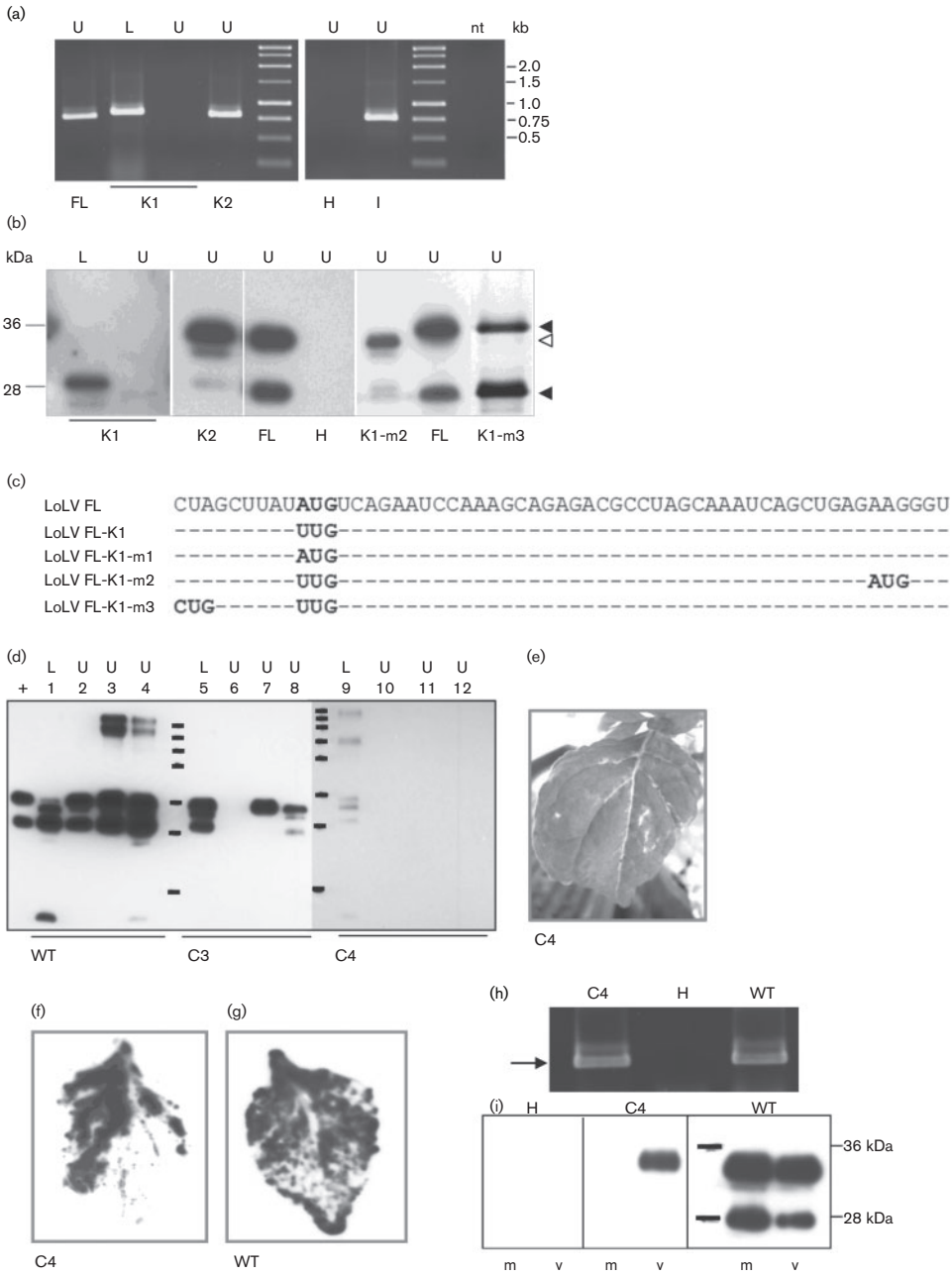

Fig. 2. (a) One-step RT-PCR of total RNA extracted (21 days p.i.) from L, lower (inoculated) leaves, or U, young upper leaves of *N. benthamiana*, transcript-inoculated with FL (WT), K1 and K2 mutants, to detect replication. Ethidium bromide-stained 1 % agarose gel; H, healthy *N. benthamiana*; I, LoLV-infected *N. benthamiana*; molecular size markers are shown on the right; nt, no-template PCR. (b) Western blot of total protein extracts (21 days p.i.) from L and U leaves, to detect CP expression. Right panel, CP expression of LoLV-K1 revertants K1-m2 and K1-m3, showing a lower-molecular-mass CP (open arrowhead) and the typical LoLV double CP pattern (filled arrowheads). Molecular size markers are shown on the left. (c) Nucleotide sequences (RNA) of LoLV variants surrounding AUG1. LoLV FL, WT infectious clone, AUG1 of 33 kDa CP shown in bold type; LoLV FL-K1, mutation AUG→UUG in bold type; LoLV FL-K1-m1, 2 and 3, the three revertant viruses, with mutated/reverted nucleotides in bold. (d) Western blots, total protein extracts from L and U leaves. Time-course following transcript inoculations of WT clone, C3 and C4 mutants. The same quantity of total protein was loaded. +, LoLV-infected plant tissue. WT: (lanes 1–4), 17, 17, 72, 120 days p.i. C3 (lanes 5–8), 17, 17, 72, 120 days p.i.; C4 (lanes 9–12), 14, 50, 120, 160 days p.i. (e) Localized systemic symptoms on *N. benthamiana* inoculated with LoLV-C4 transcripts (approx. 100 days p.i.). (f) Squash-blot of asymptomatic fully developed upper leaf of *N. benthamiana* inoculated with LoLV-C4 transcripts (45 days p.i.). Note irregular pattern associated with major veins. (g) Same as (e), but inoculated with WT LoLV-US1. Note lower signal over veins. (h) RT-PCR to detect replication in whole leaves (45 days p.i.): C4, LoLV-C4 mutant transcripts; H, non-inoculated plant; WT, LoLV-US1. The arrow indicates the 806 bp amplicon. (i) Western blot of total protein leaf extracts enriched in vascular tissue (v) or intraveinal lamina (m) of the same samples as (g). Molecular size markers are indicated.

restore translation of a larger CP while still maintaining expression of the 28 kDa CP (Fig. 2c); these were one true reversion restoring the WT AUG (K1-m1; Fig. 2b), and two second-site reversions. In second-site revertant K1-m2, a point mutation (AAG→AUG) was present in frame 42 nt after the mutated UUG, yielding the abnormal 31 kDa CP (sequence-predicted size, 30.2 kDa; Fig. 2b, c). In the other second-site revertant, K1-m3, no new AUG was found; the original AUG→UUG mutation was maintained, but a CP of about the WT size was present in Western blotting. In this case, a point mutation (CUA→CUG) was detected, creating an alternative start codon (CUG) in frame nine bases before the original AUG (K1-m3; Fig. 2b, c), a situation already described for other viruses (Shirako, 1998; James *et al.*, 2007; Koh *et al.*, 2006). Systemic infectivity and stability of each revertant clone were retained following mechanical transmission through multiple passages; sequences of K1-m2 and K1-m3 from symptomatic upper leaves have been verified by RT-PCR and sequencing after nine and eight mechanical passages, respectively. The introduced mutations were conserved and the ORF analysis was unchanged. Expression of a significant proportion of the original N-terminal cTP signal sequence is apparently crucial for systemic infection.

Ablation of putative internal initiation of the 28 kDa CP affects systemic infection, but does not prevent production of the 28 kDa CP

Western blotting from LoLV-K2-infected young leaves (21 days p.i.) mainly showed expression of the 33 kDa CP, but low amounts of the 28 kDa CP were clearly present in infected tissues, especially in late infections (Fig. 2b, lane K2). The infection could be mechanically transmitted repetitively to other plants, with stable single 33 kDa CP expression evolving with time into a double CP pattern, with a low proportion of the 28 kDa CP. To rule out the possibility that the 28 kDa CP was translated from the mutated alternative start codon TTG (UUG), an infectious clone C3 with ATG2 mutated to CCC (Fig. 1c) was tested in *N. benthamiana* by transcript inoculation and verified by sequencing; C3 and K2 had similar behaviour (Fig, 2b, d) suggesting that the low level of the 28 kDa CP observed in K2 and C3 infections resulted from proteolytic cleavage rather than regeneration of an internal initiation codon by reversion (or possible expression from UUG).

Failure to produce the 28 kDa CP via cleavage significantly delays systemic movement and alters symptom expression

In order to address the origin of 28 kDa CP by proteolytic cleavage of 33 kDa CP, an infectious clone pTOPO-LoLV-C4 was generated (Fig. 1c) to mutate the predicted cleavage between amino acids V_{42} and A_{43} of the 33 kDa CP sequence. Four amino acid substitutions at the putative cleavage site, in addition to ATG2 mutation to CCC, yielded clone C4, predicted to be unable to produce 28 kDa CP either by direct translation or by proteolytic cleavage (mutation verified by sequencing and maintained through mechanical inoculations). Following transcript inoculation, clone C4 induced pinpoint necrotic local lesions on *N. benthamiana* in which virus particles were detected (Fig. 3b). In three separate experiments, systemic symptoms were not apparent until about 60 days p.i., when white necrotic vein-netting symptoms were observed in some leaves. These symptoms first appeared on leaves subtending axillary branches, and later on some newly developing upper leaves (Fig. 2e).

RT-PCR performed at 45 days p.i. on extracts from young entire symptomless leaves amplified viral RNA (Fig. 2h) but, surprisingly, Western blot analysis (samples from interveinal leaf lamina) was not able to detect any CP, even at 160 days p.i. (Fig. 2d). Total protein extracts from leaf samples (symptomless or showing necrotic vein netting, 45 days p.i.) enriched in vascular tissue (mainly class I and II veins; Riechmann *et al.*, 1999) or in interveinal mesophyll of the leaf were then tested. Interestingly, the 33 kDa CP, the only CP produced, was detected exclusively in vein-enriched fraction of leaves showing white veinal necrosis; with WT LoLV-FL, both CPs could be readily detected also in the interveinal mesophyll-enriched tissue (Fig. 2i). Analogous leaves were tested by squash-blot on PVDF membranes, and probed with LoLV-specific antiserum; CP was shown to be associated primarily with the major veins (Fig. 2f), distinct from the interveinal distribution in the control LoLV-FL infection (Fig. 2g). Absence of the 28 kDa CP, produced from either internal initiation or proteolytic cleavage of the cTP, may inhibit phloem unloading of LoLV. The observed whitening/necrosis at veinal sites may reflect membrane clogging following abnormal C4 CP–chloroplast interactions.

Transmission electron microscopy (TEM) shows that the N-terminal sequence is also required for virus particle formation and underlines the peculiarity of mutant C4

Immunosorbent electron microscopy (ISEM) assays were performed on *N. benthamiana* inoculated with transcripts of LoLV mutants (K1, K2, C3 and C4) to determine their ability to form virions. Virus particles were trapped by LoLV-specific antiserum from local lesions of K2, C3 and C4 plants (lacking AUG2; Fig. 3a, b). Only globular/fibrous-like structures were trapped from local lesions of K1 plants (expressing 28 kDa CP only; Fig. 3d). No similar structures were observed by ISEM of healthy controls (Fig. 3c), suggesting that the globular/fibrous structures might contain aggregated 28 kDa CP. In young upper leaves, no virus particles or globular/fibrous structures were detected in K1 plants, whereas virus particles were found in K2, C3 and WT LoLV-infected plants; with C4, only a few fragile virus particles were detected (data not shown).

The histopathology produced by the mutated viral clones in local lesions collected from developmentally similar infected plants was examined by TEM. In tissues infected with LoLV-FL and K2 infectious clones, many infected cells

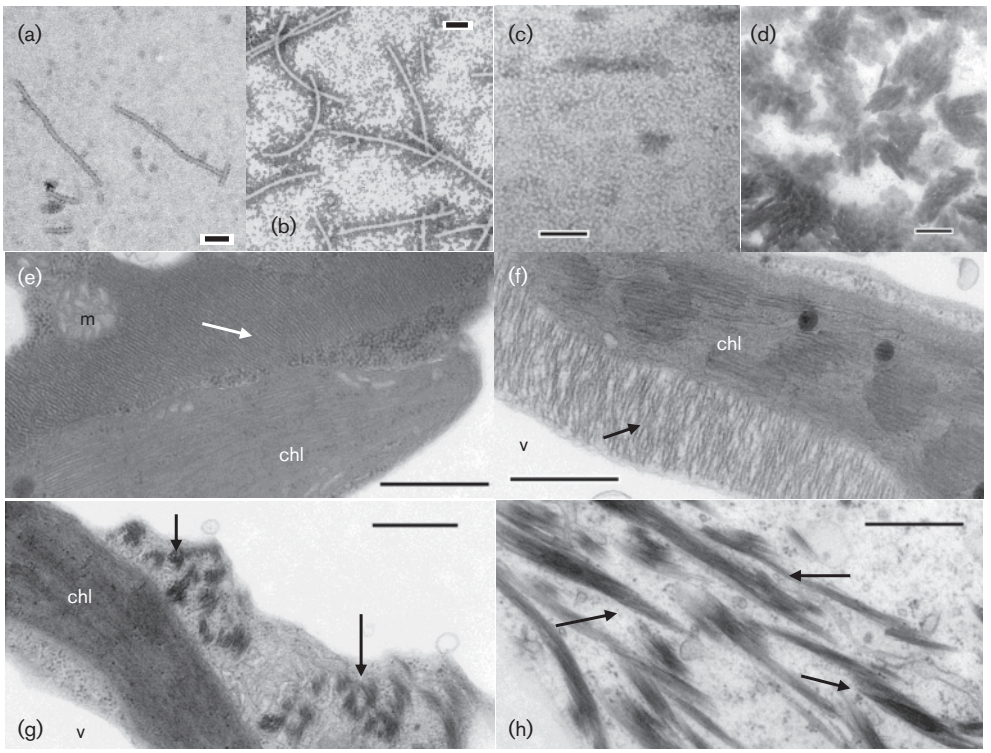

Fig. 3. TEM. (a–d) ISEM preparations from leaves inoculated with (a) C3, (b) C4 and (d) K1 mutants (23 days p.i.), and (c) healthy *N. benthamiana* tissue as negative control. Trapping and decoration with LoLV-specific antiserum. Bars, 100 nm. (e–h) Thin sections obtained from local infection (18 days p.i.) of (e) FL and (f) mutant K2 [virus particles (arrows) are observed in the cytoplasm]; (g, h) mutant K1: only elongated fibres (arrows) and no virus particles were observed. chl, Chloroplast; v, vacuole; m, mitochondrion. Bars, 500 nm.

were observed with large bundles of virus particles in the cytoplasm, mainly between chloroplast outer membranes and the vacuole membrane (Fig. 3e, f). No differences could be detected between particles formed by FL and K2. Thin sections from leaves inoculated with mutant K1 transcripts revealed only small, electron-dense bundles of fibrous material, without obvious association with either chloroplasts or vacuolar membrane, and no typical particles (Fig. 3g, h). Young leaves of C4-infected plants showed no sign of mesophyll cell damage apart from some chloroplasts showing electron-dense inclusions and disorganized structure (data not shown); no bundles of virus particles were observed in mesophyll tissue. This is consistent with the unusual localized, vein-restricted symptoms observed only with LoLV-C4 (Fig. 2e).

Cell-to-cell and systemic movement of GFP-tagged LoLV mutants

To investigate the movement of mutant clones K1, K2 and C4 further, the respective mutant CPs were substituted into a LoLV infectious clone engineered to express GFP as an added gene (GFP–FL; A. M. Vaira, H.-S. Lim & J. Hammond, unpublished data). All mutated infectious clones replicated and formed local lesions in transcript-inoculated leaves of *N. benthamiana*. Laser-scanning confocal microscopy (LSCM) revealed areas expressing GFP on the adaxial side of the leaves. GFP–FL, GFP–K2 and GFP–C4 were able to produce local lesions visible at the abaxial side of the leaves and to colonize areas around ribs. However, GFP–K1 was only able to spread within the epidermal layer on the inoculated (adaxial) side of the leaf (Fig. 4a–f), and was restricted to the inoculated leaves. GFP–FL established systemic infections more slowly and with milder symptoms than LoLV–WT, and was detected by LSCM in the lamina of upper leaves, including cells above, but generally not within, major veins (Fig. 4g); GFP–K2 was similar to GFP–FL (data not shown). In contrast, GFP–C4 was restricted primarily to localized areas within major veins, with little spread into the adjacent epidermis (Fig. 4h). Thus, a functional N-terminal cTP domain seems to be required for the virus to cross cellular boundaries and for efficient phloem loading/unloading. To address this hypothesis, we examined differential subcellular localization of the 33 and 28 kDa CPs.

Effect of the N-terminal sequence on subcellular localization of the LoLV CPs

Fusions of the 33 kDa CP and the 28 kDa CP to the N terminus of DsRed showed strikingly different patterns of

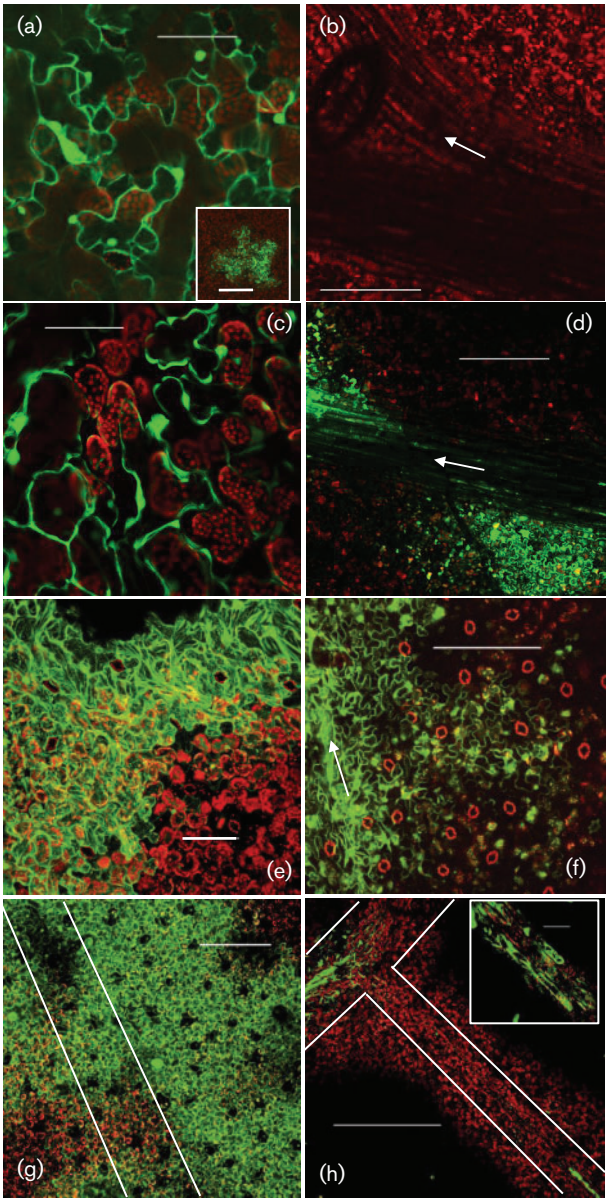

Fig. 4. (a–f) GFP-tagged LoLV clones were inoculated to the adaxial leaf surface, and fluorescence was observed (local lesions, 2–49 days p.i.; upper leaves to 83 days p.i.) by LSCM. MIP images of a *z*-stack from the top of the epidermis into the mesophyll are shown. GFP expression is shown in green; chloroplast autofluorescence is shown in red. Bars: (a, c, e) 100 μm; (f) 200 μm; (b, d and small inset in a) 500 μm. Arrows in (b, d, f) indicate veins. (a, b) K1–GFP. (a) Small local lesion (see lower magnification inset) at adaxial site. (b) No GFP expression was detected at the abaxial side. (c, d) K2–GFP. Local lesion visible at adaxial (c) and abaxial (d) surface; note (d) association of lesion with vein. (e, f) C4–GFP. Local lesion visible at adaxial (e) and crossing vein at abaxial (f) surface. (g) FL–GFP expression in abaxial epidermis across vein (marked in white) of systemic leaf (53 days p.i.). Bar, 200 μm. (h) Localized C4–GFP fluorescence at branch of major vein within systemically infected leaf (50 days p.i.); note significant fluorescence in larger vein (upper left) and at a distance in side branch (lower right). (inset) Localized C4–GFP fluorescence in a major vein within systemically infected leaf (50 days p.i.); here no epidermal fluorescence was detected. Both images are from the abaxial surface. Bars, 500 μm (inset, 100 μm).

localization following transient expression in *N. benthamiana*. The 33 kDa CP–DsRed fusion has the cTP exposed at the N terminus, whereas 28 kDa CP–DsRed completely lacks the cTP. LSCM from the adaxial side revealed that the 33 kDa CP–DsRed was confined almost exclusively to the mesophyll layer in the proximity of chloroplasts, with no obvious accumulation in the overlying epidermis (Fig. 5a). In contrast, the 28 kDa CP–DsRed formed small foci of varying sizes in both epidermal and mesophyll cells; no association with chloroplast or peripheral membranes was visible (Fig. 5b). The presence of cTP in the CP N terminus appears to be required for the virus to invade the mesophyll successfully, probably through targeting to chloroplasts.

Homologous CP interactions require the N-terminal sequence

To detect possible homologous interaction between LoLV CP subunits *in vivo*, glutathione *S*-transferase (GST)–33kDaCP fusion and the 33 or 28 kDa free CPs were co-agroinfiltrated separately, to allow protein interaction during transient expression in plant cells. Notably, immunoblot analyses of crude protein extracts prior to the addition of the glutathione beads indicated that the GST–33kDaCP fusion and the free 33 and 28 kDa CPs were expressed at similar levels (Fig. 5c). As discussed, this phenomenon is probably due to the double-expression strategy for 28 kDa CP *in vivo*.

Analysis of the eluted samples (Fig. 5d) revealed that the GST–33kDaCP fusion binds only to free 33 kDa CP and not to the 28 kDa CP, indicating that the N-terminal sequence of LoLV CP is required for homologous interaction.

Self-interaction of the 33 kDa CP was confirmed by bimolecular fluorescence complementation (BiFC) assay in agroinfiltrated *N. benthamiana* leaves. eYFP fluorescence was observed at the periphery of epidermal cells infiltrated with pSPYNE173-33 kDa CP/pSPYCEM-33 kDa CP (Fig. 5e). No eYFP fluorescence was detected with equivalent combinations of 28 kDa–28 kDa or 28 kDa–33 kDa CPs (Fig. 5f, g) or in negative controls (Fig. 5h), confirming the key role of the N-terminal cTP in homologous interactions.

Conclusions

CPs of RNA viruses are remarkably multifunctional proteins (Callaway *et al.*, 2001; Ozeki *et al.*, 2009; Cao *et al.*, 2010; Tatineni *et al.*, 2011). The 5′ region of the

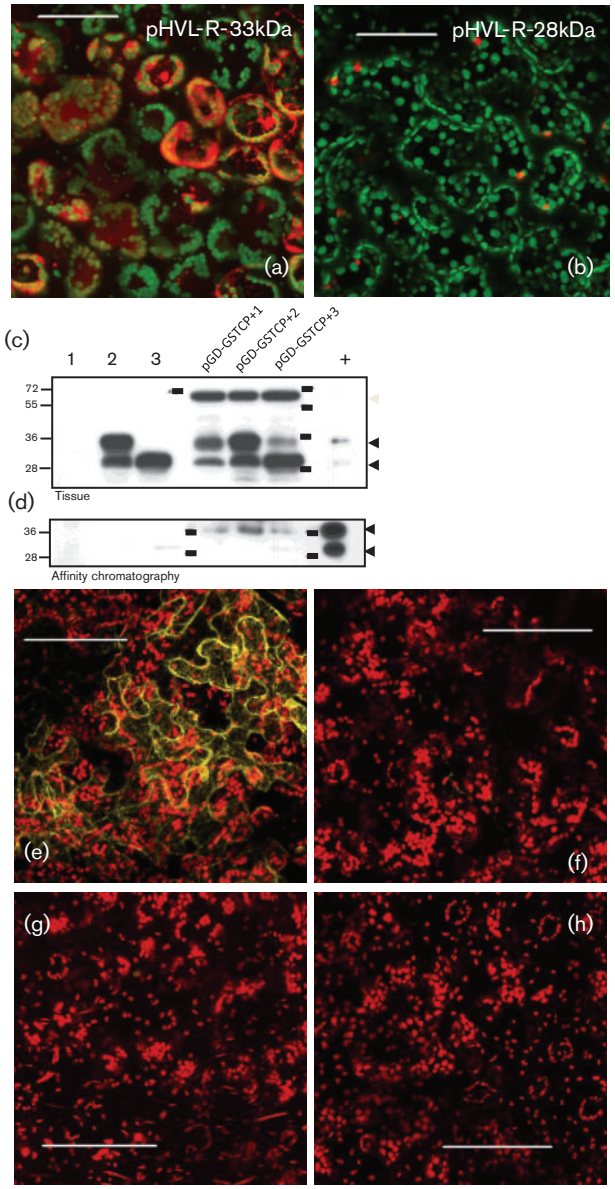

Fig. 5. (a, b) Subcellular localization by LSCM of LoLV CP–DsRed fusion proteins (2–3 days p.a.). MIP images of a *z*-stack from the top of the epidermis into the mesophyll; chloroplast autofluorescence is shown in green. Bars, 100 μm. (a) pHVL-R-33 kDa CP expressing 33 kDa–DsRed. (b) pHVL-R-28 kDa CP expressing 28 kDa–DsRed. (c) SDS-PAGE and Western blotting of total proteins from leaf tissue agroinfiltrated with (1) pGD vector (negative control); (2) pGD-33kDaCP; (3) pGD-28kDaCP, each co-agroinfiltrated with pGD-GST-33kDaCP (pGD-GSTCP). (d) Samples as in (c), following chromatography on glutathione–Sepharose affinity resin. Note that 33 kDa but not 28 kDa CP bound to GST–33kDaCP *in vivo*. (e–h) BiFC assay visualized *in vivo* by LSCM at 3 days p.a. following transient expression. (e) pSPYCEM-33 kDa/pSPYNE173-33 kDa; the interaction is visualized in epidermal cells by fluorescence complementation of YFP (yellow fluorescence). (f) pSPYCEM-28 kDa/pSPYNE173-28 kDa; (g) pSPYCEM-33 kDa/pSPYNE173-28 kDa; (h) pSPYCEM-33 kDa/pSPYCEM-33 kDa (negative control), no interaction detected. MIP images are shown. Chloroplast autofluorescence is shown in red. Bar, 100 μm.

LoLV CP ORF is strictly required for effective infection and, in addition to translation of the 33 kDa CP, its sequence allows two distinct strategies to produce CPs of approximately 28 kDa. Proteolytic cleavage of the 33 kDa CP (LoLV-FL, K2 and C3) produces systemic symptoms and yields a Δ42-N-terminal CP through a process involving interaction with chloroplasts. Additionally, a Δ48-N-terminal CP can be expressed from internal 'in-frame' AUG2 (LoLV-FL, probably by leaky scanning) and is possibly involved in virus stability. The LoLV-K1 mutant lacking AUG1 is unable to form virions in the absence of 33 kDa CP, whereas mutants lacking AUG2 (LoLV-K2, LoLV-C3, LoLV-C4) can form virions. Localization studies by LSCM and BiFC and the GFP-expressing clones indicate that the 48 aa CP N-terminal domain promotes the crossing of tissue boundaries, mesophyll/chloroplast targeting and phloem loading for systemic infection, as well as CP homologous interaction and virus particle formation. When only the 33 kDa CP is expressed, C4–GFP is limited in systemic movement and remains largely associated with class I and II veins, rather than the class III vein network, considered the principal site of unloading of potato virus X (genus *Potexvirus*) from the phloem (Roberts *et al.*, 1997).

The presence of a cTP in the N-terminal domain, reported previously for the genus *Tombusvirus* (Xiang *et al.*, 2006), implies a key role of chloroplasts in LoLV infection. In studies to be presented elsewhere, we have identified subcellular targeting and potential host interactions (A. M. Vaira, H.-S. Lim, G. R. Bauchan & J. Hammond, in preparation). Strikingly, an effect on cell-to-cell movement, similar to LoLV mutant K1 and associated with chloroplast targeting, was recently observed for mutations of *Alternanthera* mosaic virus TGB3 protein (Lim *et al.*, 2010). The vascular system required for systemic viral movement is embedded within the mesophyll of the leaf lamina; thus, targeting of chloroplasts by movement-associated viral proteins may represent a crucial early step towards systemic invasion of the host.

METHODS

Virus isolate and plant material. LoLV US1 (Vaira *et al.*, 2008) was maintained by mechanical inoculation on *N. benthamiana* using 1 % K_2HPO_4 and carborundum powder as an abrasive. Plants were grown in an insect-proof greenhouse at 25 °C, under a 14 h light regime.

Construction of LoLV infectious clones. All enzymes, kits or reagents were used according to their manufacturers' instructions. All primers used are listed in Table S1, available in JGV Online.

Sequence analyses were performed using DNASTAR-Lasergene v6 (DNASTAR Inc.), ORF Finder at the NCBI website and NEBcutter v. 2.0 (Vincze *et al.*, 2003). Additional analyses utilized amino acid sequence-based prediction tools hosted at the Center for Biological Sequence Analysis, Technical University of Denmark (Emanuelsson

et al., 2007). Total RNA was isolated from LoLV-infected *N. benthamiana* leaves using an RNeasy Mini kit (Qiagen) and was used to generate full-length cDNA by AffinityScript Multiple Temperature Reverse Transcriptase (Stratagene) using a modified oligo(dT)$_{26}$ primer (MF22p3-R); LoLV 5′ and 3′ sequences were amplified by PCR with *Pfu*Ultra II FusionHS DNA polymerase (Stratagene); the 5′ non-coding region primer included a T7 promoter sequence upstream of LoLV nt 1. The LoLV 3′ sequence was obtained similarly and the two PCR products were cloned in TOPO-blunt vector (Invitrogen) and combined at a unique *Spe*I site (Fig. 1a). Seven full-length clones were transcribed *in vitro* and transcripts were inoculated onto *N. benthamiana*; plants were assayed at 21 days p.i. by RT-PCR and Western blotting (Fig. 1b). The full-length LoLV sequence was also cloned into pUC18 using a similar two-step procedure; six full-length clones were obtained. The viral sequence of pUC18-LoLVFL-cl7 (10377 bp, fully sequenced) and pTOPO-LoLVFL-cl2 (11261 bp, partially sequenced) were used as references in this study. All experiments were carried out with pTOPO-LoLVFL-cl2 or derivatives.

***In vitro* transcription of LoLV infectious clones.** Thirty micrograms of *Swa*I-linearized plasmid DNA was used per 50 µl transcription reaction, using T7 RNA polymerase (Petty *et al.*, 1989). Transcripts were ethanol-precipitated, resuspended in 20 µl GKP buffer (Petty *et al.*, 1989) and inoculated to *N. benthamiana* plants.

Mutation of ATG1, ATG2 and of the putative cleavage site (aa V_{42}–A_{43}) of the CP ORF in infectious clones. A subclone, pUC18-LoLVeng (Fig. 1a), containing the *Avr*II/*Bbv*CI fragment of the LoLV genome (comprising the 3′ end of TGB2, TGB3 and the 5′ end of CP) was prepared as a template for site-directed mutagenesis through PCR (Lu, 2005) to alter the two CP ATGs separately. The fragment was amplified using primers LoLVeng1/LoLVeng2 with *Hin*dIII/*Eco*RI adaptor arms for pUC18 cloning. The LoLV-specific sequence of the pUC18-LoLVeng clone was verified by sequencing. Primer pairs of 25 bp each, complementary to each other and carrying point mutation TTG instead of ATG in the middle of the sequence, were prepared for each CP ATG and inverse PCR was performed with pUC18-LoLVeng as template. Purified PCRs were subjected to *Dpn*I restriction to eliminate unmutated template. After purification, 1 µl DNA was used for bacterial transformation.

The mutated *Avr*II/*Bbv*CI fragment of each of the two selected clones was substituted separately into infectious clone pTOPO-LoLV-FL-cl2 to obtain pTOPO-LoLV-K1 and pTOPO-LoLV-K2 (Fig. 1a, c).

Two other LoLV infectious clone mutants were obtained using overlap-extension PCR (Wurch *et al.*, 1998) to mutate ATG2→CCC (pTOPO-LoLV-C3) and ATG2→CCC plus PVAT→CRYQ (at the putative chloroplast cleavage site; pTOPO-LoLV-C4) (Fig. 1c).

The modified portion of all clones was sequenced to verify the substituted regions. Clones were then linearized with *Swa*I and *in vitro*-transcribed.

Insertion of K1, K2 and C4 mutations into an infectious LoLV clone expressing GFP. The K1, K2 and C4 mutations were inserted by sequence substitution into a tissue-traceable pTOPO-LoLV-FL infectious clone expressing eGFP as an extra gene (A. M. Vaira, H.-S. Lim & J. Hammond, unpublished data). *Cla*I/*Bbv*CI fragments obtained by *Pfu*/PCR from the pTOPO-LoLV-K1, K2 and C4 infectious clones (spanning the CP subgenomic promoter plus the 5′ CP sequence bearing the appropriate mutations) were subcloned between an engineered unique *Cla*I site (immediately following the GFP gene) and the unique *Bbv*CI site (Fig. 1a) to substitute the corresponding sequences. The mutated clones were verified by sequencing. Clones pTOPO-LoLV-K1 : EGFP, pTOPO-LoLV-K2 : EGFP and pTOPO-LoLV-C4 : EGFP were linearized, *in vitro*-transcribed and transcripts were inoculated to *N. benthamiana*. Fluorescence was observed *in vivo* by LSCM in inoculated and upper leaves (7–60 days p.i.) or by UV photography of whole plants using an LAS-1000 luminescence imaging system (Fuji).

Subcellular localization of 28 and 33 kDa CPs. The 33 and 28 kDa CP ORFs were PCR-amplified as *Xho*I/*Kpn*I fragments, *Xho*I/*Kpn*I-digested, subcloned into pHVL-R (Lim *et al.* 2010) as CP–DsRed fusions and verified by sequencing the fusion junction region. *Agrobacterium tumefaciens* EHA105 competent cells were transformed by standard protocols (Johansen & Carrington, 2001) and transient expression of all clones was evaluated by LSCM in *N. benthamiana* leaves at 2 or 3 days post-agroinfiltration (p.a.). Fusion protein expression was verified by Western blotting.

Western- and squash-blot detection of CP, and LoLV-specific RT-PCR. Total protein extraction was performed by using CellLytic P Cell Lysis reagent (Sigma) according to the manufacturer's protocol, with Halt Protease Inhibitor Cocktail (Thermo Scientific) added, or by Smash buffer (Deng *et al.*, 2007), boiling for 10 min and centrifugation at 13 200 r.p.m. for 10 min to pellet insoluble material. Supernatant containing the solubilized protein fraction was separated by SDS-PAGE (12 % acrylamide). Gels were stained (Simply Blue Safe Stain; Invitrogen) according to the manufacturer's instructions, or were blotted to PVDF membrane (Immobilon-P; Millipore) and incubated with LoLV-specific polyclonal antiserum (Vaira *et al.*, 2008). The Δ42 N-terminal CP and the Δ48 N-terminal CP (both approx. 28 kDa) were indistinguishable in size under our electrophoresis conditions.

For squash-blots, leaves were frozen with liquid nitrogen prior to pressing between sheets of Immobilon-P, and processed as for Western blots.

Detection of LoLV infection/replication was performed using one-step RT-PCR as described previously (Vaira *et al.*, 2008), producing a diagnostic 806 bp amplicon.

Detection of fluorescent protein expression in *N. benthamiana*. LSCM using a Zeiss LSM 710 microscope was used for detection of GFP, DsRed and chloroplast autofluorescence as described previously (Lim *et al.*, 2010). eYFP was excited at 514 nm (argon laser, MBS458/514 filter set) and emission was detected at 520–550 nm.

Zeiss Zen 2009 software was used to obtain the images with maximum intensity projection (MIP) of *z*-stacks (1 µm slices, 25–80 focal planes) of leaves from the top of the epidermis into the mesophyll.

ISEM and thin sectioning of leaf tissue for TEM analysis. ISEM was performed on healthy and infected *N. benthamiana* sap using LoLV-specific antiserum coated grids, essentially according to Milne & Luisoni (1975, 1977). For observation of tissue thin sections, segments (approx. 2 × 1 mm) were excised from healthy or infected leaves of *N. benthamiana* and embedded in resin (Lawson & Hearon, 1974). ISEM grids and ultrathin sections were examined with a JEOL 100CX II transmission electron microscope equipped with an AMT HR digital camera system.

GST–LoLV 33 kDa CP fusion protein construct and GST pull-down assay. The CP sequence was amplified as an *Xho*I/*Bam*HI fragment and subcloned in pGD : GST (Deng *et al.*, 2007) in order to obtain expression of the GST–33kDaCP fusion. The 33 and 28 kDa CPs were introduced separately into pGD (Goodin *et al.*, 2002) in the same manner. Binary plasmids were transformed into *A. tumefaciens* EHA105 by standard protocols. Transient expression in *N. benthamiana* was performed by agroinfiltration (at OD_{600}=0.6) with pGD vector alone or expressing free 33 or 28 kDa CPs, and co-agroinfiltration with

pGD-GST-33kDaCP; pGD-p19 (Bragg & Jackson, 2004) was included at a 1 : 10 ratio in all infiltrations as described previously (Lim *et al.*, 2009). Agroinfiltrated tissue (3 days p.a.) was checked by Western blotting for expression of desired proteins, and was macerated (about 1.6 g in 6 ml) in STE buffer plus protease-inhibitor cocktail (Thermo Scientific) and subjected to protein purification and affinity chromatography using glutathione–Sepharose 4B affinity resin (GE Healthcare). The GST-pulled-down proteins were eluted from the resin, boiled and analysed by SDS-PAGE (12 % acrylamide) and Western blotting as above.

BiFC. The LoLV 33 and 28 kDa genes were subcloned into both pSPYCE(M) and pSPYNE173, as fusions with, respectively, C- and N-terminal eYFP domains (Waadt *et al.*, 2008). Constructs were agroinfiltrated in all combinations as described previously and eYFP fluorescence was observed at 3 days p.a. by LSCM. Fusion protein expression was verified by Western blotting as described above.

ACKNOWLEDGEMENTS

We thank Dr Rosemarie Hammond for helpful discussions and Dr Lev Nemchinov for comments on the manuscript.

REFERENCES

Adams, M. J., Candresse, T., Hammond, J., Kreuze, J. F., Martelli, G. P., Namba, S., Pearson, M. N., Ryu, K. H. & Vaira, A. M. (2012). Family *Alphaflexiviridae*. In *Virus Taxonomy: Ninth Report of the International Committee on Taxonomy of Viruses*, pp. 904–919. Edited by A. M. Q. King, M. J. Adams, E. B. Carstens & E. J. Lefkowitz. San Diego, CA: Elsevier Academic Press.

Bragg, J. N. & Jackson, A. O. (2004). The C-terminal region of the *Barley stripe mosaic virus* γb protein participates in homologous interactions and is required for suppression of RNA silencing. *Mol Plant Pathol* **5**, 465–481.

Bruun-Rasmussen, M., Madsen, C. T., Johansen, E. & Albrechtsen, M. (2008). Revised sequence of foxtail mosaic virus reveals a triple gene block structure similar to potato virus X. *Arch Virol* **153**, 223–226.

Callaway, A., Giesman-Cookmeyer, D., Gillock, E. T., Sit, T. L. & Lommel, S. A. (2001). The multifunctional capsid proteins of plant RNA viruses. *Annu Rev Phytopathol* **39**, 419–460.

Cao, M., Ye, X., Willie, K., Lin, J., Zhang, X., Redinbaugh, M. G., Simon, A. E., Morris, T. J. & Qu, F. (2010). The capsid protein of *Turnip crinkle virus* overcomes two separate defense barriers to facilitate systemic movement of the virus in *Arabidopsis*. *J Virol* **84**, 7793–7802.

Deng, M., Bragg, J. N., Ruzin, S., Schichnes, D., King, D., Goodin, M. M. & Jackson, A. O. (2007). Role of the sonchus yellow net virus N protein in formation of nuclear viroplasms. *J Virol* **81**, 5362–5374.

Emanuelsson, O., Brunak, S., von Heijne, G. & Nielsen, H. (2007). Locating proteins in the cell using TargetP, SignalP and related tools. *Nat Protoc* **2**, 953–971.

Goodin, M. M., Dietzgen, R. G., Schichnes, D., Ruzin, S. & Jackson, A. O. (2002). pGD vectors: versatile tools for the expression of green and red fluorescent protein fusions in agroinfiltrated plant leaves. *Plant J* **31**, 375–383.

Hammond, R. W. & Hammond, J. (2010). *Maize rayado fino virus* capsid proteins assemble into virus-like particles in *Escherichia coli*. *Virus Res* **147**, 208–215.

Hammond, R. W. & Ramirez, P. (2001). Molecular characterization of the genome of *Maize rayado fino virus*, the type member of the genus *Marafivirus*. *Virology* **282**, 338–347.

James, D., Varga, A. & Croft, H. (2007). Analysis of the complete genome of peach chlorotic mottle virus: identification of non-AUG start codons, *in vitro* coat protein expression, and elucidation of serological cross-reactions. *Arch Virol* **152**, 2207–2215.

Johansen, L. K. & Carrington, J. C. (2001). Silencing on the spot. Induction and suppression of RNA silencing in the *Agrobacterium*-mediated transient expression system. *Plant Physiol* **126**, 930–938.

Joshi, C. P., Zhou, H., Huang, X. Q. & Chiang, V. L. (1997). Context sequences of translation initiation codon in plants. *Plant Mol Biol* **35**, 993–1001.

Koh, D. C., Wang, X., Wong, S. M. & Liu, D. X. (2006). Translation initiation at an upstream CUG codon regulates the expression of *Hibiscus chlorotic ringspot* virus coat protein. *Virus Res* **122**, 35–44.

Lawson, R. H. & Hearon, S. S. (1974). Ultrastructure of carnation etched ring virus-infected *Saponaria vaccaria* and *Dianthus caryophyllus*. *J Ultrastruct Res* **48**, 201–215.

Li, R., Maroon-Lango, C., Mock, R. & Hammond, J. (2008). Lolium latent virus. In *Characterization, Diagnosis and Management of Plant Viruses*, vol. 4, pp. 215–220. Edited by G. P. Rao, C. Bragard & B. S. M. Lebas. Houston, TX: Studium Press.

Lim, H. S., Bragg, J. N., Ganesan, U., Ruzin, S., Schichnes, D., Lee, M. Y., Vaira, A. M., Ryu, K. H., Hammond, J. & Jackson, A. O. (2009). Subcellular localization of the *Barley stripe mosaic virus* triple gene block proteins. *J Virol* **83**, 9432–9448.

Lim, H. S., Vaira, A. M., Bae, H., Bragg, J. N., Ruzin, S. E., Bauchan, G. R., Dienelt, M. M., Owens, R. A. & Hammond, J. (2010). Mutation of a chloroplast-targeting signal in *Alternanthera* mosaic virus TGB3 impairs cell-to-cell movement and eliminates long-distance virus movement. *J Gen Virol* **91**, 2102–2115.

Lu, Q. (2005). Seamless cloning and gene fusion. *Trends Biotechnol* **23**, 199–207.

Milne, R. G. & Luisoni, E. (1975). Rapid high-resolution immune electron microscopy of plant viruses. *Virology* **68**, 270–274.

Milne, R. G. & Luisoni, E. (1977). Rapid immune electron microscopy of virus preparations. *Methods Virol* **6**, 265–281.

Mise, K., Tsuge, S., Nagao, K., Okuno, T. & Furusawa, I. (1992). Nucleotide sequence responsible for the synthesis of a truncated coat protein of brome mosaic virus strain ATCC66. *J Gen Virol* **73**, 2543–2551.

Ozeki, J., Hashimoto, M., Komatsu, K., Maejima, K., Himeno, M., Senshu, H., Kawanishi, T., Kagiwada, S., Yamaji, Y. & Namba, S. (2009). The N-terminal region of the *Plantago asiatica mosaic virus* coat protein is required for cell-to-cell movement but is dispensable for virion assembly. *Mol Plant Microbe Interact* **22**, 677–685.

Petty, I. T. D., Hunter, B. G., Wei, N. & Jackson, A. O. (1989). Infectious barley stripe mosaic virus RNA transcribed *in vitro* from full-length genomic *c*DNA clones. *Virology* **171**, 342–349.

Riechmann, J. L., Ito, T. & Meyerowitz, E. M. (1999). Non-AUG initiation of *AGAMOUS* mRNA translation in *Arabidopsis thaliana*. *Mol Cell Biol* **19**, 8505–8512.

Roberts, A. G., Cruz, S. S., Roberts, I. M., Prior, D., Turgeon, R. & Oparka, K. J. (1997). Phloem unloading in sink leaves of *Nicotiana benthamiana*: comparison of a fluorescent solute with a fluorescent virus. *Plant Cell* **9**, 1381–1396.

Robertson, N. L., French, R. & Morris, T. J. (2000). The open reading frame 5A of foxtail mosaic virus is expressed in vivo and is dispensable for systemic infection. *Arch Virol* **145**, 1685–1698.

Satyanarayana, T., Gowda, S., Ayllón, M. A. & Dawson, W. O. (2004). Closterovirus bipolar virion: evidence for initiation of assembly by minor coat protein and its restriction to the genomic RNA 5′ region. *Proc Natl Acad Sci U S A* **101**, 799–804.

Shirako, Y. (1998). Non-AUG translation initiation in a plant RNA virus: a forty-amino-acid extension is added to the N terminus of the soil-borne wheat mosaic virus capsid protein. *J Virol* **72**, 1677–1682.

Solovyev, A. G., Novikov, V. K., Merits, A., Savenkov, E. I., Zelenina, D. A., Tyulkina, L. G. & Morozov, S. Y. (1994). Genome characterization and taxonomy of *Plantago asiatica* mosaic potexvirus. *J Gen Virol* **75**, 259–267.

Tatineni, S., Van Winkle, D. H. & French, R. (2011). The N-terminal region of wheat streak mosaic virus coat protein is a host- and strain-specific long-distance transport factor. *J Virol* **85**, 1718–1731.

Vaira, A. M., Maroon-Lango, C. J. & Hammond, J. (2008). Molecular characterization of Lolium latent virus, proposed type member of a new genus in the family *Flexiviridae*. *Arch Virol* **153**, 1263–1270.

Vincze, T., Posfai, J. & Roberts, R. J. (2003). NEBcutter: A program to cleave DNA with restriction enzymes. *Nucleic Acids Res* **31**, 3688–3691.

Waadt, R., Schmidt, L. K., Lohse, M., Hashimoto, K., Bock, R. & Kudla, J. (2008). Multicolor bimolecular fluorescence complementation reveals simultaneous formation of alternative CBL/CIPK complexes *in planta*. *Plant J* **56**, 505–516.

Wurch, T., Lestienne, F. & Pauwels, P. J. (1998). A modified overlap extention PCR method to create chimeric genes in the absence of restriction enzymes. *Biotechnol Tech* **12**, 653–657.

Xiang, Y., Kakani, K., Reade, R., Hui, E. & Rochon, D. (2006). A 38-amino-acid sequence encompassing the arm domain of the *Cucumber necrosis virus* coat protein functions as a chloroplast transit peptide in infected plants. *J Virol* **80**, 7952–7964.